Chapter 2
The Chemical Batch Reactor

List of Principal Symbols

A	reactant A
B	reactant B
c	mass heat capacity [$\mathrm{J\,kg^{-1}\,K^{-1}}$]
C	concentration [$\mathrm{mol\,m^{-3}}$]
DPh	aggregate dimers
E_a	activation energy [$\mathrm{J\,mol^{-1}}$]
ΔE_R	internal energy change of reaction [$\mathrm{J\,mol^{-1}}$]
F	formaldehyde
F_V	volumetric flow rate [$\mathrm{m^3\,s^{-1}}$]
F_M	molar flow rate [$\mathrm{mol\,s^{-1}}$]
ΔH_R	molar enthalpy change of reaction [$\mathrm{J\,mol^{-1}}$]
I	reaction intermediate
k_0	preexponential factor [$(\mathrm{mol\,m^{-3}})^{1-n}\,\mathrm{s^{-1}}$]
k_c	rate constant [$(\mathrm{mol\,m^{-3}})^{1-n}\,\mathrm{s^{-1}}$]
K_{eq}	equilibrium constant
m	mass [kg]
MPh	mono- and di-methylolphenols
n	order of reaction
N	number of moles [mol]
N_C	number of species
N_R	number of reactions
P	reaction product
Ph	phenol
PPh	polyphenols
R	reaction rate [$\mathrm{mol\,m^{-3}\,s^{-1}}$]
$\mathcal{R}$	universal gas constant [$\mathrm{J\,mol^{-1}\,K^{-1}}$]
$\mathrm{R^\bullet}$	radical species
S	heat transfer area [$\mathrm{m^2}$]
$\mathcal{S}$	selectivity
t	time [s]

F. Caccavale et al., *Control and Monitoring of Chemical Batch Reactors*,
Advances in Industrial Control,
DOI 10.1007/978-0-85729-195-0_2, © Springer-Verlag London Limited 2011

t_b batch time [s]
t_P residence time [s]
T temperature [K]
TMPh trimethylolphenol
U overall heat transfer coefficient [J m^{-2} K^{-1} s^{-1}]
V volume [m^3]
X degree of conversion

Greek Symbols
ρ density [kg m^{-3}]
υ stoichiometric coefficient

Subscripts and Superscripts
a ambient conditions
A reactant A
ad adiabatic conditions
B reactant B
in inlet
j jacket
max maximum
min minimum
out outlet
r reactor
0 initial value
° reference value

2.1 Ideal Chemical Reactors

Chemical reactions occur almost everywhere in the environment; however, a chemical reactor is defined as a device properly designed to let reactions occur under controlled conditions toward specified products. To a visual observation, chemical reactors may strongly differ in dimensions and structure; nevertheless, in order to derive a mathematical model for their quantitative description, essentially two major features are to be considered: the mode of operation and the quality of mixing.

Therefore, the analysis of the main object of this book, namely, the batch chemical reactor, can start by considering the different ideal chemical reactors. In fact, ideal reactors are strongly simplified models of real chemical reactors [10], which however capture the two major features mentioned above. These models can be classified according to the mode of operation (i.e., discontinuous vs. continuous) and to the quality of mixing (i.e., perfect mixing vs. no mixing). The three resulting ideal reactors are sketched in Fig. 2.1.

The discontinuous stirred reactor (Batch Reactor, BR, Fig. 2.1(a)) corresponds to a closed thermodynamic system, whereas the two continuous reactors (Continuous Stirred Tank Reactor, CSTR, Fig. 2.1(b), and Plug Flow Reactor, PFR, Fig. 2.1(c))

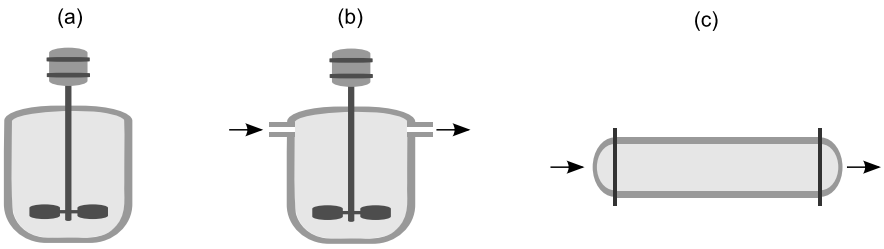

Fig. 2.1 Ideal reactors: BR (**a**), CSTR (**b**), and PFR (**c**)

are open systems. In industry, discontinuous operations are well suited for the production of valuable products through rather complex reactions and allow one to drive the reaction pattern by controlling the temperature, whereas continuous operations in (approximately) steady-state conditions are typical of large productions, usually based on a more simple chemistry.

The two extreme hypotheses on mixing produce lumped models for the fluid dynamic behavior, whereas real reactors show complex mixing patterns and thus gradients of composition and temperature. It is worthwhile to stress that the fluid dynamic behavior of real reactors strongly depends on their physical dimensions. Moreover, in ideal reactors the chemical reactions are supposed to occur in a single phase (gaseous or liquid), whereas real reactors are often multiphase systems. Two simple examples are the gas–liquid reactors, used to oxidize a reactant dissolved in a liquid solvent and the fermenters, where reactions take place within a solid biomass dispersed in a liquid phase. Real batch reactors are briefly discussed in Chap. 7, in the context of suggestions for future research work.

Those simplified models are often used together with simplified overall reaction rate expressions, in order to obtain analytical solutions for concentrations of reactants and products. However, it is possible to include more complex reaction kinetics if numerical solutions are allowed for. At the same time, it is possible to assume that the temperature is controlled by means of a properly designed device; thus, not only adiabatic but isothermal or nonisothermal operations as well can be assumed and analyzed.

The main ideas of chemical kinetics are reviewed in the next section; for the sake of completeness, a brief account is given here of the performance of continuous reactors as compared to BR, which is the object of the present book.

Whereas the operation of batch reactors is intrinsically unsteady, the continuous reactors, as any open system, allow for at least one reacting steady-state. Thus, the control problem consists in approaching the design steady-state with a proper startup procedure and in maintaining it, irrespective of the unavoidable changes in the operating conditions (typically, flow rate and composition of the feed streams) and/or of the possible failures of the control devices. When the reaction scheme is complex enough, the continuous reactors behave as a nonlinear dynamic system and show a complex dynamic behavior. In particular, the steady-state operation can be hindered by limit cycles, which can result in a marked decrease of the reactor performance. The analysis of the above problem is outside the purpose of the present text;

nevertheless, a few interesting observations can be made on the simple steady-state operation.

Apparently, the PFR differs more strongly from the BR, since it is a continuous reactor with no mixing. Nevertheless, when the PFR is described in the Eulerian mode, it appears as made of infinitesimal reaction volumes, dV, behaving as differential batch reactors, since they remain in the reactor for a residence (or permanence) time $t_P = V_r/F_V$ (where V_r is the reactor volume, and F_V is the volumetric flow rate passing through the reactor) and do not experience relative mixing. Thus, this reactor can be described by the same equations of the batch reactor, when t_P is considered in lieu of the time variable t. It is worth remarking that, for any fixed reactor volume, t_P can be changed by changing F_V, e.g., in order to optimize the reactor performance.

For the perfectly mixed continuous reactor, the CSTR, the ratio V_r/F_V only represents the mean residence time, $t_{P,av}$; however, it is still possible to compare the performance of the CSTR with the performance of the BR by letting the mean residence time $t_{P,av} = t$. Interestingly, when the reaction rate shows a positive dependence on reactants concentration, the BR is more effective than the CSTR. This is because the batch reactor experiences all the system compositions between initial and final values, whereas the CSTR operates at the final composition, where the reaction rate is smaller (under the above hypotheses). Finally, one can compare the two continuous reactors under steady-state conditions. The CSTR allows a more stable operation because of back-mixing, which however reduces the chemical performance, whereas the PFR is suitable for large heat transfer but suffers from larger friction losses.

2.2 The Rate of Chemical Reactions

Chemical reactions change the molecular structure of matter, thus resulting in the destruction of some chemical species (reactants) and in the formation of different ones (products). The relevant quantities of reactants and products involved in the reaction are strictly determined by stoichiometry, which states a law of proportionality deriving from the mass conservation of the single elements. Often, the stoichiometric coefficients are imposed to be constant during the reaction; however, this is not true in most real systems. When variable stoichiometric coefficients are observed, the system cannot be described by a single reaction.

With reference to a simple reaction with constant stoichiometric coefficients, and unless otherwise specified, the reaction rate R [moles time^{-1} volume^{-1}] measures the specific velocity of destruction of those reactants (and of formation of those products) that appear with unitary stoichiometric coefficients. The reaction rates of each other component are proportional to R according to their stoichiometric coefficients.

In general, the rate of a chemical reaction can be expressed as a function of chemical composition and temperature. This function usually takes the form of a power law with respect to reactant concentrations and of an exponential function in the inverse absolute temperature. As an example, the rate R of conversion of A and

B in the reaction

$$\mathrm{A} + \mathrm{B} \rightarrow \text{products} \tag{2.1}$$

can be expressed as

$$R = k_{\mathrm{c}}(T_{\mathrm{r}}) C_{\mathrm{A}}^{n_{\mathrm{A}}} C_{\mathrm{B}}^{n_{\mathrm{B}}} = k_0 \exp\left(-\frac{E_{\mathrm{a}}}{\mathcal{R} T_{\mathrm{r}}}\right) C_{\mathrm{A}}^{n_{\mathrm{A}}} C_{\mathrm{B}}^{n_{\mathrm{B}}}, \tag{2.2}$$

where C_{A} and C_{B} are the molar concentrations of reactants, n_{A} and n_{B} are the orders of reaction ($n = n_{\mathrm{A}} + n_{\mathrm{B}}$ being the overall reaction order), $k_{\mathrm{c}}(T_{\mathrm{r}})$ is the rate constant, k_0 is the preexponential factor, E_{a} is the activation energy, $\mathcal{R}$ is the universal gas constant, and T_{r} is the absolute reaction temperature. Since, on varying temperature from 0 to ∞, the S-shaped function $\exp(-E_{\mathrm{a}}/\mathcal{R}T_{\mathrm{r}})$, known as Arrhenius law or Arrhenius term, ranges from 0 to 1, the preexponential factor k_0 represents the limit of k_{c} as $T_{\mathrm{r}} \rightarrow \infty$.

Function (2.2) can be considered as an empirical model used to best fit the experimental concentration-time data. In practice, laws different from (2.2) are also encountered, especially when dependence on the concentration is considered; however, a simple theory based on the kinetic theory of gases can only explain the simplest of these empirical rate laws. The general idea of this theory is that reaction occurs as a consequence of a collision between adequately energized molecules of reactants. The frequency of collision of two molecules can explain simple reaction orders, namely the schemes

$$\mathrm{A} + \mathrm{B} \rightarrow \text{products} \quad (R_{\mathrm{A}} \propto C_{\mathrm{A}} C_{\mathrm{B}}), \tag{2.3}$$

$$\mathrm{A} + \mathrm{A} \rightarrow \text{products} \quad \left(R_{\mathrm{A}} \propto C_{\mathrm{A}}^2\right), \tag{2.4}$$

$$\mathrm{A} + \text{third body} \rightarrow \text{products} \quad (R_{\mathrm{A}} \propto C_{\mathrm{A}}), \tag{2.5}$$

where *third body* stands for any molecule with constant concentration. Any collision involving more than two molecules is very unlikely and must be neglected.

On the other hand, the effective collision concept can explain the Arrhenius term on the basis of the fraction of molecules having sufficient kinetic energy to destroy one or more chemical bonds of the reactant. More accurately, the formation of an *activated complex* (i.e., of an unstable reaction intermediate that rapidly degrades to products) can be assumed. Theoretical expressions are available to compute the rate of reaction from thermodynamic properties of the activated complex; nevertheless, these expression are of no practical use because the detailed structure of the activated complexes is unknown in most cases. Thus, in general the kinetic parameters (rate constants, activation energies, orders of reaction) must be considered as unknown parameters, whose values must be adjusted on the basis of the experimental data.

Chemical reactions occurring because of a single kinetic act, i.e., because of a single collision between two molecules, are defined as *elementary reactions*. More complex laws of dependence on concentrations can be explained by complex reaction mechanisms, i.e., by the idea that most reactions occur as a sequence of many elementary reactions, linked in series or in parallel. As an example, the following

simple reaction mechanism, made out of two reaction steps in series, can explain a fractionary reaction order. Let us consider the reaction

$$\mathrm{A} + \mathrm{B} \rightarrow \mathrm{P}, \tag{2.6}$$

for which a first-order behavior with respect to each reactant can be foreseen on the basis of the collision theory. Nevertheless, suppose that this reaction is not caused by a single collision, but with the following mechanism: first, reactant A is in equilibrium with a reaction intermediate I since both direct and inverse reactions are very fast:

$$\mathrm{A} \rightleftharpoons 2\,\mathrm{I}, \tag{2.7}$$

then, I reacts with B producing P,

$$\mathrm{I} + \mathrm{B} \rightarrow \mathrm{P}. \tag{2.8}$$

By applying the result (2.3) to reaction (2.8) and introducing the equilibrium constant, K_{eq}, for the reaction (2.7), defined as

$$K_{\mathrm{eq}} = \frac{C_{\mathrm{I}}^2}{C_{\mathrm{A}}}, \tag{2.9}$$

one obtains

$$R = k_{\mathrm{c}} C_{\mathrm{I}} C_{\mathrm{B}} = k_{\mathrm{c}} (K_{\mathrm{eq}} C_{\mathrm{A}})^{1/2} C_{\mathrm{B}}. \tag{2.10}$$

The apparent rate constant in (2.10), which is obtained by multiplying a true rate constant k_{c} and the square root of an equilibrium constant, K_{eq}, can show a law of dependence on temperature different from the simple Arrhenius law. In some cases, even a negative temperature dependence can be observed. Moreover, if both mechanisms (2.6) and (2.7)–(2.8) are active in parallel, the observed reaction rate is the sum of the single rates, and an effective reaction order variable from $1/2$ to 1 can be observed with respect to reactant A. Variable and fractionary reaction orders can be also encountered in heterogeneous catalytic reactions as a consequence of the adsorption on a solid surface [6].

Very fast reactions, such as combustion reactions, are very often characterized by chain mechanisms activated by very reactive species, such as radicals. First, radicals, $\mathrm{R}_1^{\bullet}$, are formed by an opening reaction involving the reactant A,

$$\mathrm{A} \longrightarrow 2\,\mathrm{R}_1^{\bullet}; \tag{2.11}$$

then, the chain is propagated by a loop of reactions that continuously produces the final product P and regenerates the radicals:

$$\mathrm{R}_1^{\bullet} + \mathrm{B} \longrightarrow \mathrm{P} + \mathrm{R}_2^{\bullet}, \tag{2.12}$$

$$\mathrm{R}_2^{\bullet} + \mathrm{A} \longrightarrow \mathrm{P} + \mathrm{R}_1^{\bullet}. \tag{2.13}$$

Moreover, branching reaction mechanisms can take place when at least one reaction leads to multiplication of radicals, such as

$$R_1^{\bullet} + A \longrightarrow P + R_2^{\bullet} + R_3^{\bullet}. \tag{2.14}$$

In this case, the fast increase of concentration of radicalic species can result in the loss of control of the reaction (runaway) and in the explosion of the system. This radicalic runaway may be strongly enhanced by linked thermal effects that are discussed in more details in Chap. 4.

Kinetic mechanisms involving multiple reactions are by far more frequently encountered than single reactions. In the simplest cases, this leads to reaction schemes in series (at least one component acts as a reactant in one reaction and as a product in another, as in (2.7)–(2.8)), or in parallel (at least one component acts as a reactant or as a product in more than one reaction), or to a combination series-parallel. More complex systems can have up to hundreds or even thousands of intermediates and possible reactions, as in the case of biological processes [12], or of free-radical reactions (combustion [16], polymerization [4]), and simple reaction pathways cannot always be recognized. In these cases, the true reaction mechanism mostly remains an ideal matter of principle that can be only approximated by reduced kinetic models. Moreover, the values of the relevant kinetic parameters are mostly unknown or, at best, very uncertain.

The model reduction procedure must be adapted to the use of the simplified models and to the availability of experimental data needed to evaluate the unknown parameters, as discussed in Chap. 3. In general, more complex models are used for the design of the reactor and for the simulation of the entire process, whereas more simplified models are best fit for feedback control. In the following chapters it is shown that fairly accurate results are obtained when a strongly simplified kinetic model is used for control and fault diagnosis purposes.

2.3 The Ideal Batch Reactor

A more quantitative analysis of the batch reactor is obtained by means of mathematical modeling. The mathematical model of the ideal batch reactor consists of mass and energy balances, which provide a set of ordinary differential equations that, in most cases, have to be solved numerically. Analytical integration is, however, still possible in isothermal systems and with reference to simple reaction schemes and rate expressions, so that some general assessments of the reactor behavior can be formulated when basic kinetic schemes are considered. This is the case of the discussion in the coming Sect. 2.3.1, whereas nonisothermal operations and energy balances are addressed in Sect. 2.3.2.

2.3.1 Conservation of Mass

An independent mass balance can be written for each chemical species (or component of the reacting system) in the reactor. Let $N_i = V_r C_i$ denote the molar quantity of the ith species, where V_r is the volume of the reactor. Assuming a single reaction with rate R, the rate of change of the molar quantity, $\dot{N}_i = dN_i/dt$ [moles time^{-1}], must be equal to the rate of reaction taken with the proper algebraic sign, i.e.,

$$\dot{N}_i = \upsilon_i R V_r, \tag{2.15}$$

where υ_i is the stoichiometric coefficient of the ith component, taken negative if this component is a reactant and positive if it is a product. Since the reaction rate is a function of concentrations, it is useful to explicate the accumulation term as

$$\dot{N}_i = V_r \dot{C}_i + C_i \dot{V}_r, \tag{2.16}$$

which, under the assumption of constant volume of reaction, gives

$$\dot{C}_i = \upsilon_i R. \tag{2.17}$$

It appears that, in the case of constant volume BR, the reaction rate is strictly linked to the time derivatives of concentrations. This result, which cannot be generalized to different reactors, may be however useful to visualize the concept of reaction rate.

When multiple reactions occur simultaneously, the right-hand side of (2.17) is replaced by a sum of reaction terms

$$\dot{C}_i = \sum_{j=1}^{N_R} \upsilon_{i,j} R_j, \tag{2.18}$$

where N_R is the total number of reactions and $\upsilon_{i,j}$ is the stoichiometric coefficient of component i in reaction j, again taken negative if component i is a reactant in reaction j, positive if it is a product, and null if it is not involved. Hence, if N_C species are involved in the reaction, a set of N_C equations in the form (2.18) can be written, eventually in compact matrix form.

Table 2.1 reports some of the most classical basic reaction schemes encountered in chemical engineering, together with the explicit expressions of the isothermal concentration profiles as functions of time. The effect of the reaction order can be evaluated by considering the first three cases in Table 2.1; by applying the corresponding rate laws, the curves shown in Fig. 2.2 are obtained. To allow an easier comparison, the values of the rate constants have been chosen so as to obtain the same C_A at an arbitrary batch time t_b.

The zero-order kinetics is characterized by a linear concentration profile, which is however unrealistic at very large reaction times, since it produces a negative reactant concentration; this result confirms that a zero-order reaction derives from a complex reaction mechanism that cannot be active at very low reactant concentrations. On increasing the reaction order, the reaction is faster at the highest concentration values

Table 2.1 Simple reaction schemes

No.		Kinetic scheme	Integrated BR model equation
1	zero order	$A \xrightarrow{k_{c0}} P$	$C_A = C_{A0} - k_{c0}t$
2	first order	$A \xrightarrow{k_{c1}} P$	$C_A = C_{A0}\exp(-k_{c1}t)$
3	second order	$A \xrightarrow{k_{c2}} P$	$C_A = \dfrac{C_{A0}}{1+k_{c2}t}$
4	equilibrium	$A \underset{k_{cA}}{\overset{k_{cB}}{\rightleftharpoons}} B$	$C_A = \frac{C_{A0}}{1+K_{eq}}[1-\exp(-(k_{cA}+k_{cB})t)]$
5	parallel	$A \xrightarrow{k_{cP1}} P_1$	$C_A = C_{A0}\exp(-(k_{cP1}+k_{cP2})t)$
		$A \xrightarrow{k_{cP2}} P_2$	$C_{P1} = C_{A0}\frac{k_{cP1}}{k_{cP1}+k_{cP2}}[1-\exp(-(k_{cP1}+k_{cP2})t)]$
6	series	$A \xrightarrow{k_{cI}} I \xrightarrow{k_{cP}} P$	$C_A = C_{A0}\exp(-k_{cI}t)$
			$C_I = C_{A0}\frac{k_{cI}}{k_{cP}-k_{cI}}[\exp(-k_{cI}t)-\exp(-k_{cP}t)]$
7	multiple series	$A \rightarrow \cdots \rightarrow P$	
8	series-parallel	$A \xrightarrow{k_{cI}} I \xrightarrow{k_{cP}} P$	$C_A = C_{A0}\exp(-(k_{cI}+k_{cS})t)$
		$A \xrightarrow{k_{cS}} P$	$C_I = C_{A0}\frac{k_{cI}}{k_{cP}-k_{cS}-k_{cI}}[\exp(-(k_{cI}+k_{cS})t)-\exp(-k_{cP}t)]$

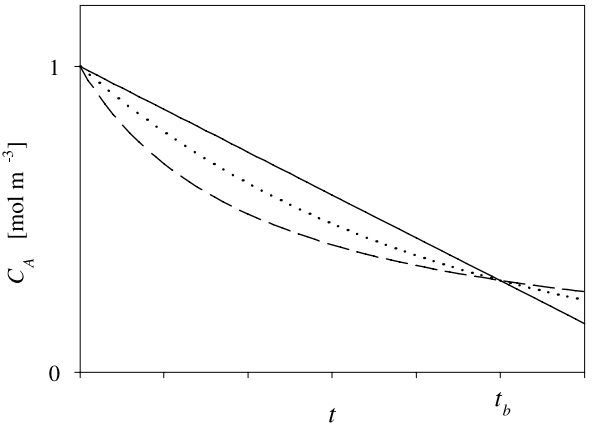

Fig. 2.2 Time histories of C_A in a batch reactor for zero (*continuous line*), first (*dotted line*) and second (*dashed line*) order reaction rates and $C_{A0} = 1\ \text{mol m}^{-3}$

and slower at the lowest. Nevertheless, the effect of the reaction order is rather small, so that, in many cases, the simpler first-order behavior is considered to be an adequate approximation. Thus, unit reaction orders for each reactant are assumed in the following when dealing with more complex reaction schemes.

In the equilibrium limited case (fourth row in Table 2.1, Fig. 2.3), it is possible to simulate the constant C_B/C_A ratio imposed by thermodynamics by introducing the inverse reaction $B \rightarrow A$. In this case, the reaction is not complete, and an asymptotic behavior is observed for both reactant and product.

In the parallel reaction scheme (fifth row in Table 2.1), competition is observed between the two reactions when only one of the products is required and the other one is a secondary undesired or a low value product. In this case, the degree of

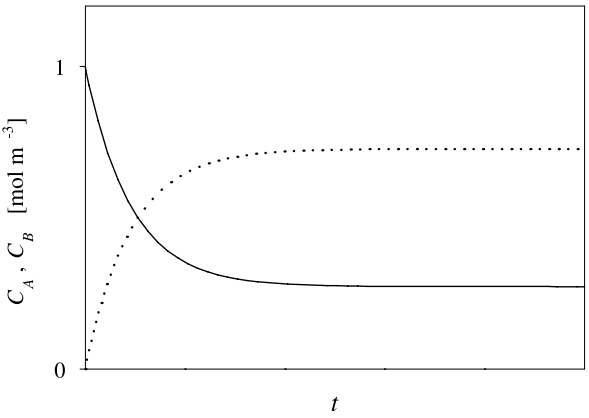

Fig. 2.3 Time histories of C_A (*continuous line*) and C_B (*dotted line*) in a batch reactor for the equilibrium limited reaction. Initial conditions are: $C_{A0} = 1$ mol m^{-3} and $C_{B0} = 0$ mol m^{-3}

conversion of the reactant, defined as

$$X = \frac{N_{A0} - N_A}{N_{A0}} = \frac{C_{A0} - C_A}{C_{A0}}, \tag{2.19}$$

where the expression in terms of concentrations holds for constant-volume reactors, is unable to describe the product distribution, so that the selectivity concept must be introduced. As an example, the selectivity to P_1 is defined, for unit stoichiometric coefficients, as

$$\mathcal{S}_{P_1} = \frac{C_{P_1}}{C_{A0} - C_A}. \tag{2.20}$$

Finally, when chemical kinetics contrasts with equilibrium, the parallel scheme is not trivial, since one of the products can be favored in the early stages of the batch cycle by faster kinetics and hindered in the later stages by unfavorable equilibrium. Such a case is shown in Fig. 2.4 for parallel reactions of A to P_1 via an equilibrium limited reaction and to P_2 via an irreversible reaction.

In the reaction scheme in series (sixth row in Table 2.1), the required product is often the intermediate I, and its concentration has a maximum at time t^*, which can be taken as the optimal batch time, t_b. When the system follows a first-order kinetics not affected by chemical equilibrium (Fig. 2.5), it can be easily shown that t^* depends on the values of the rate constants through the following expression:

$$t^* = \frac{\ln(k_{cP}/k_{cI})}{k_{cP} - k_{cI}}. \tag{2.21}$$

It is worth remarking that, in real cases, the simple criterion $t_b = t^*$, based on the system's selectivity to the desired product, must be modified to account for the cost of operation (including separation between products and unreacted reactants) and the gross added value related to the transformation of reactants into products.

It is also interesting to note that the concentration–time curve of the final product P has a typical shape with zero derivative at $t = 0$ and an asymptotic trend at very

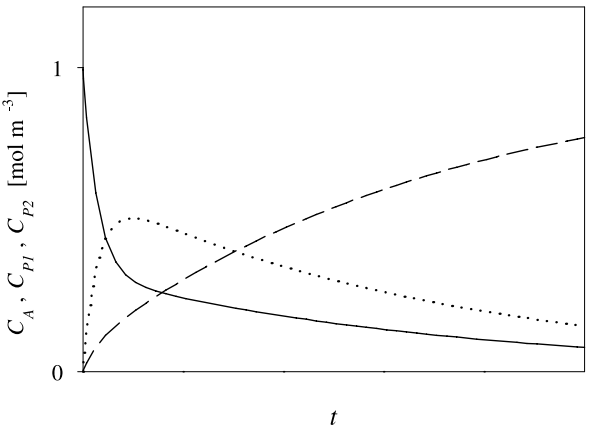

Fig. 2.4 Time histories of C_A (*continuous line*), C_{P1} (*dotted line*), and C_{P2} (*dashed line*) in a batch reactor for parallel reactions of A producing P_1, via an equilibrium limited reaction, and P_2, via an irreversible reaction. Initial conditions are: $C_{A0} = 1$ mol m^{-3}, $C_{P10} = C_{P20} = 0$ mol m^{-3}

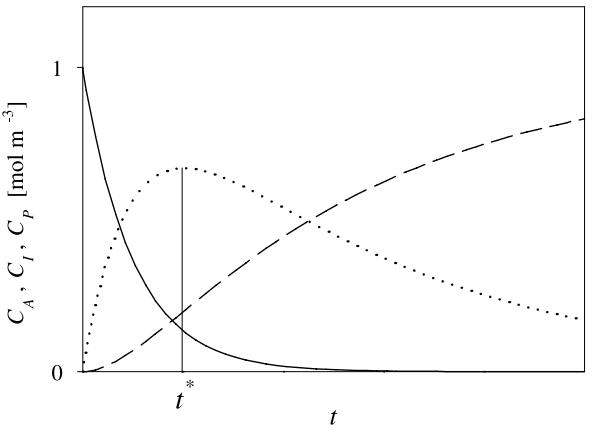

Fig. 2.5 Time histories of C_A (*continuous line*), C_I (*dotted line*), and C_P (*dashed line*) in a batch reactor for irreversible series reactions. Initial conditions are: $C_{A0} = 1$ mol m^{-3}, $C_{I0} = C_{P0} = 0$ mol m^{-3}

large times. These features are also encountered in more complex series schemes, i.e., when more than one intermediate is observed (seventh row in Table 2.1), and/or when kinetics is hindered by unfavorable equilibrium. In general, it appears that the time t^* must be considered only as a first approximation of the optimal batch time, which is computed as before on the basis of a cost analysis.

Finally, the eighth reaction mechanism in Table 2.1 includes both series and parallel reactions to the same product P. This scheme is more complete and somewhat more realistic, but it is not so much different from the series scheme, because the side parallel reaction to P only produces small changes in the shape of the concentration profiles. As an example, the initial zero derivative for C_P can be canceled.

It is also interesting to quantitatively compare the performance of a BR with those obtained by a CSTR, for which the reaction term RV_r acts as a selective stream entering or leaving the reactor; hence, the mass balance for a CSTR reads

$$F_{MA,in} = F_{V,in}C_{A,in} = F_{MA,out} + RV_r = F_{V,out}C_{A,out} + RV_r, \tag{2.22}$$

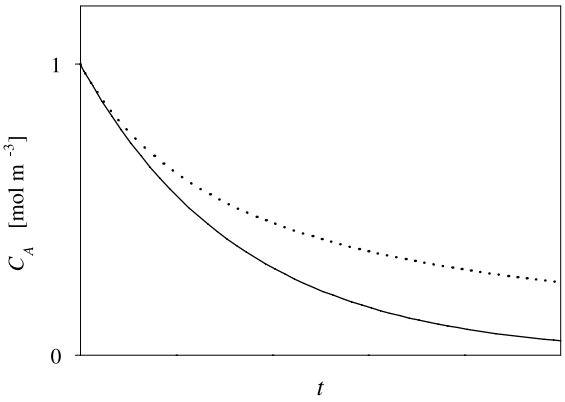

Fig. 2.6 Time histories of C_A for a first-order reaction in a BR (*continuous line*) and in a CSTR (*dotted line*). Initial condition is $C_{A0} = 1\ \text{mol m}^{-3}$

where $F_{MA,in}$ and $F_{MA,out}$ are, respectively, the inlet and outlet molar flow rates.

In the case of first-order reactions, the exit concentration of reactant A is given by

$$C_{A,out} = \frac{C_{A,in}}{1 + t_{P,av} k_c}. \tag{2.23}$$

The relevant results in Fig. 2.6 can be interpreted in the light of the considerations reported at the end of Sect. 2.1.

2.3.2 Conservation of Energy

The conservation of energy (heat balance) introduces an important element of realism into the model, i.e., the coupling of the reactor with the heating/cooling device. When the potential energy stored in chemical bonds is transformed by an exothermal chemical reaction into sensible heat, considerable thermal effects may be produced that can be quantitatively described by a proper form of the equation of energy conservation. In a batch reactor, the accumulation of internal energy is given by the difference between the heat produced by reaction and the heat exchanged with the surroundings:

$$\text{Stored Energy} = \text{Generated Heat} - \text{Exchanged Heat}. \tag{2.24}$$

A few simplified assumptions make this equation of practical utility. The left-hand side in (2.24), i.e., the rate of change of internal energy [energy time^{-1}], is simply related to the total mass m of reaction solution, to the overall constant volume specific heat capacity c_{vr} [energy mass^{-1} temperature^{-1}], and to the rate of change of reactor temperature $\dot{T}_r$. The heat generated by chemical reaction is given by the product of the specific molar energy change due to reaction, ΔE_R, and the amount of moles converted in the reactor per unit time, RV_r.

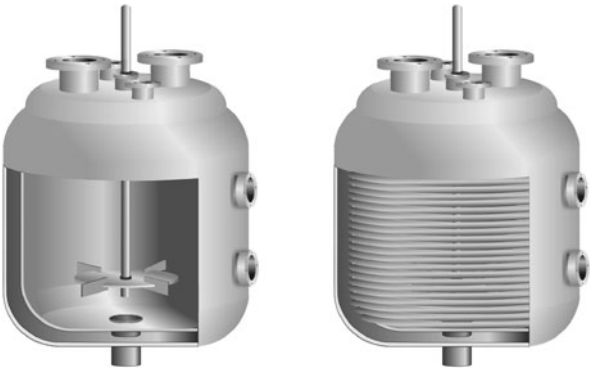

Fig. 2.7 Batch reactor with external heat exchange jacket (*left*) and coil (*right*)

The values of ΔE_R can be computed from the standard internal energy change ΔE_R^o, which refers to reactants and products in their standard states (not mixed, at 1 atm and 25°C) but also depends on temperature and, for nonideal solutions, on the heat of mixing of the components. Since a detailed description of these second-order thermal effects is beyond the purposes of a standard modeling approach, this quantity can be approximated by the standard molar enthalpy change (usually named standard heat of reaction), ΔH_R^o, which can be easily computed from available tables of standard enthalpy of formation of the individual compounds. Since ΔH_R^o is positive for endothermic reactions, a minus sign is usually introduced in the energy balance. Consistent with this simplified assumption, in liquid-phase systems the (very small) difference between the constant-pressure and constant-volume heat capacities can be neglected; hence, the heat capacity is hereafter denoted by c_r, without any further specification.

The second term on the right-hand side of (2.24) depends on the modes of heat exchange between the reactor and a heat exchange medium or the surroundings. In general, in order to accomplish the different stages of a batch operation (initial reactor heating, reaction development, and final cooling), the reactor must be provided with a properly designed device for heat exchange. A jacket or a coil, as depicted in Fig. 2.7, are suitable for heating (e.g., by using hot water or steam) and cooling (e.g., by using cold water) only for relatively small heat loads, since the exchange area is limited by the external reactor surface.

For larger heat loads, i.e., when ΔE_R and/or R and/or V_r increase, a larger heat exchange surface must be provided. A heat exchanger made out of several tubes located inside the reactor allows one to obtain a larger surface-to-volume ratio; however, its dimensions are limited by the reactor volume and by effectiveness of mixing of the reaction media. Thus, for large heat loads, an external shell and tube heat exchanger must be designed, whose dimensions do not depend on the reactor dimensions. The reaction solution circulates from the reactor to the exchanger and then back to the reactor in a closed loop; this circulating flow also produces a positive effect on the mixing of the reactor contents.

According to Newton's law of heat exchange, the heat exchanged by the reactor depends on the overall coefficient of heat exchange, U, on the heat exchange surface

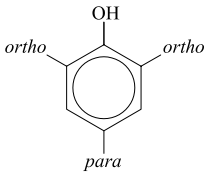

Fig. 2.8 Reactive positions on the phenolic ring

S, and on the temperature difference between the reactor and the coolant, $T_r - T_j$. In conclusion, a general form of the heat balance is given by

$$mc_r\dot{T}_r = \left(-\Delta H_R^0\right)RV_r - US(T_r - T_j). \tag{2.25}$$

For nonjacketed reactors, a further term $-U_a S(T_r - T_a)$ can be eventually added to the energy balance to account for heat losses toward reactor surroundings. Here, U_a is the overall coefficient of heat exchange with the external environment, and T_a is the external environment temperature.

When (2.25) is integrated from the initial condition $t = 0$ and $C_A = C_{A0}$ to $t \to \infty$ and $C_A \to 0$ in the case of adiabatic reactor ($US = 0$), the adiabatic temperature rise $\Delta T_{ad} = T_{ad} - T_0$ is obtained, which represents a useful measure of practical utility of the system reactivity in terms of the maximum temperature obtainable when chemical energy is entirely transformed into sensible heat.

2.4 Introducing the Case Study

In this section, the phenol–formaldehyde reaction is introduced as a case study. This reaction has been chosen because of its kinetic complexity and its high exothermicity, which poses a strong challenge for modeling and control practice. The kinetic model presented here is adopted to simulate a realistic batch chemical process; the identification, control, and diagnosis approaches developed in the next chapters are validated by resorting to this model.

Phenol (C_6H_5OH) and formaldehyde (CH_2O) can react in different ways depending on the catalyst used and the initial formaldehyde-to-phenol molar ratio. In the production of resol-type phenolic resins, in the presence of an alkaline catalyst, the reactions occurring in the system can be classified into two main types, namely, reactions of addition of methylol groups to the aromatic ring and reactions of condensation of aromatic rings to form higher molecular weight components and, finally, polymers [14].

In the alkaline solution, phenol is essentially present as phenate ion, so that the first steps of the reaction may be depicted as electrophilic additions of formaldehyde to the aromatic ring. Those attacks are essentially favored in the *-ortho* (o) and *-para* (p) positions, as sketched in Fig. 2.8, because relatively stable low activation energy intermediates can be formed; on the contrary, the attacks in the *-meta* positions are much slower and are not considered here.

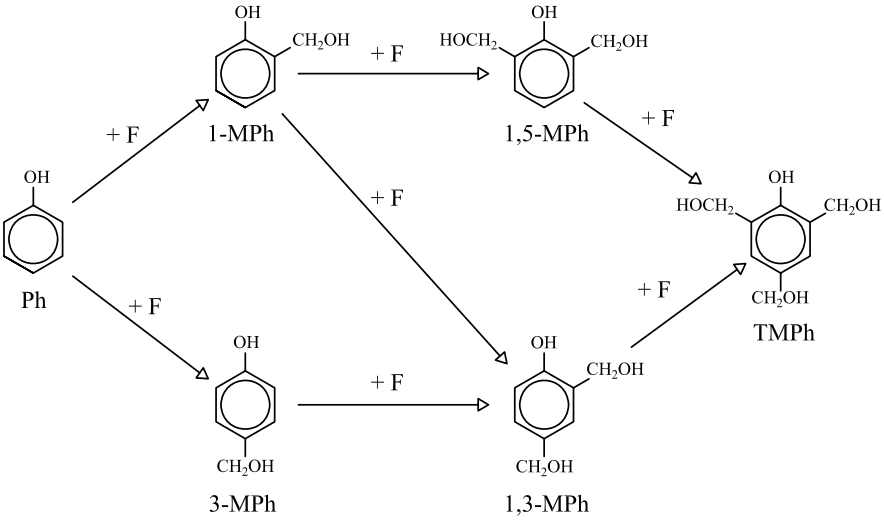

Fig. 2.9 Reactions of addition to the phenolic ring (1-MPh = o-methylolphenol, 3-MPh = p-methylolphenol, 1,5-MPh = 1,5-methylolphenol, 1,3-MPh = 1,3-methylolphenol, TMPh = 1,3,5-methylolphenol)

These reactions largely prevail in the early stages of the reaction, when both phenol and formaldehyde are present in large concentrations. This stage is characterized by the 7 reactions sketched in Fig. 2.9 and is faster than the following condensation stage; therefore, a mixture of phenol (Ph), formaldehyde (F), two mono-methylolphenols (o-methylolphenol = 1-MPh, p-methylolphenol = 3-MPh), two di-methylolphenols (1,5-methylolphenol = 1,5-MPh, 1,3-methylolphenol = 1,3-MPh), and 1,3,5-methylolphenol = trimethylolphenol = TMPh is initially formed.

The condensation reactions become important in a later stage when the concentration of the substituted phenols has increased. These reactions can occur in two different modes, as in the two examples sketched in Fig. 2.10; namely, the substituted methylol groups can react either with a nonsubstituted (free) position of a different aromatic ring (a) or with a second methylol group (b).

In the first case, the reaction produces a methylene-diphenol (MDPh), i.e., molecules in which two phenolic rings are linked by a methylene group. In the second case, the reaction produces an aromatic ether, i.e., a molecule in which two aromatic rings are linked by a dimethyl-ether group. However, these compounds are relatively unstable and rapidly decay (producing a formaldehyde molecule) to the corresponding methylene-diphenols (MDPh). Thus, the first reaction step is the rate limiting step, whereas the second one determines the final product and the total stoichiometry of the reaction.

In these reactions, a large number of two-ring isomers are formed, depending on the position of attack. In a later stage of reaction, these diphenols can undergo both addition reactions of one more methylol group on a free position of the aromatic

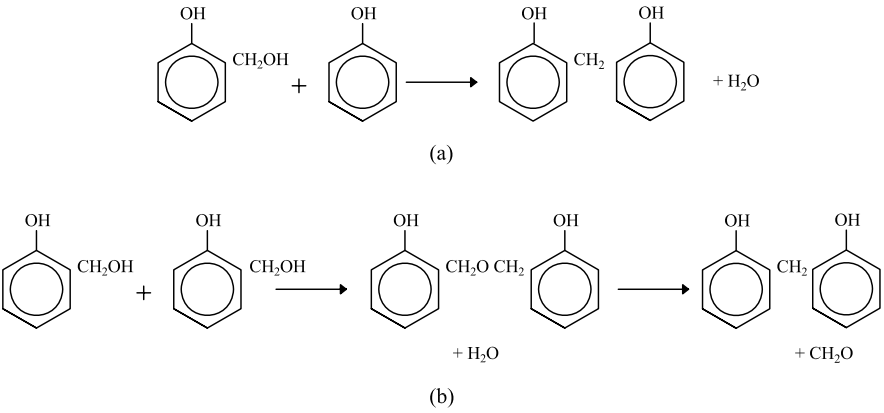

Fig. 2.10 Examples of condensation reactions: **a** condensation of methylolphenol with phenol; **b** condensation of two methylolphenols

ring and reactions of condensation to three- and four-ring molecules and finally to larger molecular weight polymers. Nevertheless, the attention is focused here on the production of TMPh, a product that has a commercial value as a prepolymer for resol-type resins; thus, the condensation reactions of higher molecular weight molecules are usually limited by quenching the system at a suitable reaction time. On the basis of the above analysis, a quantitative kinetic model is derived, as discussed in the next two sections.

2.4.1 Components

Only a few studies have tackled the problem of deriving a detailed kinetic model of the phenol–formaldehyde reactive system, mainly because of its complexity. In recent years, a generalized procedure has been reported in [11, 14] that allows one to build a detailed model for the synthesis of resol-type phenolic resins. This procedure is based on a group contribution method and virtually allows one to estimate the kinetic parameters of every possible reaction taking place in the system.

In order to develop an exhaustive kinetic model, some basic assumptions have been made. First, the two mono-methylolphenols and the two di-methylolphenols have been indicated as MPh_i (MPh_i, $i = 1, \ldots, 4$). Moreover, since the TMPh is the desired product, some simplifications have been introduced for describing the components containing more than one phenolic ring. In detail, all the diphenols having the same number of methylol groups have been considered as one single component, regardless of the position of these methylol groups. This allows one to consider in the model only 5 different aggregate methylene diphenols DPh_i ($i = 0, \ldots, 4$), where i is the number of methylol groups. In the same way, triphenols have been taken into account as just one aggregate poliphenol (PPh), whereas compounds with more than three phenolic rings have not been considered here, since the system is

usually quenched before their formation becomes detectable. Therefore, the resulting reactive scheme involves 13 chemical compounds:

- reactants: phenol (Ph) and formaldehyde (F)
- intermediates: four mono- and di-methylolphenols (MPh_i, $i = 1, \ldots, 4$)
- desired product: trimethylolphenol (TMPh)
- undesired products: five aggregate dimers (DPh_i, $i = 0, \ldots, 4$) and
- undesired product: aggregate component PPh, including all the poliphenols with three phenolic rings.

2.4.2 Reactions

A second-order kinetics has been assumed [8, 14] for all reactions included in the reaction mechanism, which is composed by the following 89 reactions:

- 7 addition reactions of formaldehyde to phenol, sketched in Fig. 2.9
- 77 condensation reactions involving two monophenolic molecules as reactants (Ph or MPh_i, $i = 1, \ldots, 4$)
- 4 addition reactions of formaldehyde to aggregate dimers; and
- 1 condensation reaction of dimers with monomers.

In order to estimate the kinetic parameters for the addition and condensation reactions, the procedure proposed in [11, 14] has been used, where the rate constant k_c of each reaction at a fixed temperature of 80°C is computed by referring it to the rate constant k_c^o at 80°C of a reference reaction, experimentally obtained. The ratio k_c/k_c^o, assumed to be temperature independent, can be computed by applying suitable correction coefficients, which take into account the different reactivity of the *-ortho* and *-para* positions of the phenol ring, the different reactivity due to the presence or absence of methylol groups and a frequency factor. In detail, the values in [11] for the resin RT84, obtained in the presence of an alkaline catalyst and with an initial molar ratio phenol/formaldehyde of 1 : 1.8, have been adopted. Once the rate constants at 80°C and the activation energies are known, it is possible to compute the preexponential factors k_0 of each reaction using the Arrhenius law (2.2).

For the molar enthalpy change of reaction, the values $\Delta H_R^o = -20.3$ kJ mol^{-1} and $\Delta H_R^o = -98.7$ kJ mol^{-1} have been used for addition and condensation reactions, respectively [9].

In the following, all the reactions included in the model are reported together with the values of the relevant kinetic parameters. Addition reactions, from 1 to 7, are reported in Table 2.2, whereas condensation reactions to the single dimers (DPh_i) are reported in Tables 2.3, 2.4, 2.5, 2.6, and 2.7; for all condensation reactions, an activation energy of 90 kJ mol^{-1} has been assumed.

It should be observed that in Table 2.3 the three nonsubstituted two-ring isomers are indicated as 1,6-MDPh, 1,8-MDPh, and 3,8-MDPh, where the numbers indicate the position of the two hydroxyl groups with respect to the methylene bridge, respectively, in the o–o, o–p, and p–p positions. Those numbers are preserved in the

Table 2.2 Addition reactions producing monomers

No.	Reaction	k_0 [m^3 mol^{-1} s^{-1}]	E_a [kJ mol^{-1}]
1	Ph + F → 1-MPh	$1.13 \cdot 10^5$	89.1
2	Ph + F → 3-MPh	$2.26 \cdot 10^5$	91.7
3	o-MPh + F → 1,5-MPh	$4.34 \cdot 10^5$	98.5
4	o-MPh + F → 1,3-MPh	$2.09 \cdot 10^5$	88.2
5	p-MPh + F → 1,3-MPh	$1.11 \cdot 10^7$	99.0
6	1,5-MPh + F → 1,3,5-MPh	$1.68 \cdot 10^2$	91.5
7	1,3-MPh + F → 1,3,5-MPh	$6.99 \cdot 10^5$	92.2

Table 2.3 Condensation reactions producing the dimers DPh_0

No.	Reaction	k_0 [m^3 mol^{-1} s^{-1}]
8	Ph + 1-MPh → 1,6-MDPh	$3.65 \cdot 10^3$
9	Ph + 1-MPh → 1,8-MDPh	$3.01 \cdot 10^3$
10	Ph + 3-MPh → 1,8-MDPh	$2.31 \cdot 10^3$
11	Ph + 3-MPh → 3,8-MDPh	$1.91 \cdot 10^3$
12	1-MPh + 1-MPh → 1,6-MDPh + F	$1.45 \cdot 10^3$
13	1-MPh + 3-MPh → 1,8-MDPh + F	$9.17 \cdot 10^2$
14	3-MPh + 3-MPh → 3,8-MDPh + F	$5.82 \cdot 10^2$

following tables and determine the numbers used to indicate the positions occupied by the methylol groups.

The four addition reactions of formaldehyde to a diphenol are reported in Table 2.8; in this case the activation energy is assumed at the value $E_a = 90$ kJ mol^{-1} as well.

Finally, the reaction no. 89 has been included with the aim of considering, for the sake of completeness, the reactions that produce higher molecular weight molecules. In fact, as discussed before, these reactions are almost negligible in the system under study, in the sense that the system behavior is almost insensitive to such reactions at the reaction times of interest. Thus, the approximate kinetic law

$$\sum_{i=1}^{4} \mathrm{MPh}_i + \sum_{i=0}^{4} \mathrm{DPh}_i \rightarrow \text{trimers}, \tag{2.26}$$

has been assumed, with a second-order kinetics, $k_0 = 9.69 \cdot 10^3$ m^3 mol^{-1} s^{-1}, which corresponds to the average value of the other condensation reactions considered, and $E_a = 90$ kJ mol^{-1}.

Table 2.4 Condensation reactions producing the dimers DPh_1

No.	Reaction	k_0 [$m^3\ mol^{-1}\ s^{-1}$]
15	Ph + 1,5-MPh → 2-M-1,6-MDPh	$2.75 \cdot 10^4$
16	Ph + 1,5-MPh → 2-M-1,8-MDPh	$2.28 \cdot 10^4$
17	Ph + 1,3-MPh → 4-M-1,6-MDPh	$1.59 \cdot 10^3$
18	Ph + 1,3-MPh → 4-M-1,8-MDPh	$1.32 \cdot 10^3$
19	Ph + 1,3-MPh → 7-M-1,8-MDPh	$2.04 \cdot 10^3$
20	Ph + 1,3-MPh → 2-M-3,8-MDPh	$1.68 \cdot 10^3$
21	1-MPh + 1-MPh → 2-M-1,6-MDPh	$2.89 \cdot 10^3$
22	1-MPh + 1-MPh → 7-M-1,8-MDPh	$1.83 \cdot 10^4$
23	1-MPh + 3-MPh → 2-M-1,8-MDPh	$3.62 \cdot 10^2$
24	1-MPh + 3-MPh → 2-M-3,8-MDPh	$5.81 \cdot 10^3$
25	1-MPh + 3-MPh → 4-M-1,6-MDPh	$1.23 \cdot 10^4$
26	3-MPh + 3-MPh → 4-M-1,8-MDPh	$1.56 \cdot 10^4$
27	1-MPh + 1,5-MPh → 2-M-1,6-MDPh + F	$1.09 \cdot 10^4$
28	1-MPh + 1,3-MPh → 4-M-1,6-MDPh + F	$6.32 \cdot 10^2$
29	1-MPh + 1,3-MPh → 7-M-1,8-MDPh + F	$8.08 \cdot 10^2$
30	3-MPh + 1,5-MPh → 2-M-1,8-MDPh + F	$6.93 \cdot 10^4$
31	3-MPh + 1,3-MPh → 4-M-1,8-MDPh + F	$4.01 \cdot 10^2$
32	3-MPh + 1,3-MPh → 2-M-3,8-MDPh + F	$5.12 \cdot 10^2$

2.5 A General Model for a Network of Nonchain Reactions

The kinetic model developed in Sect. 2.4 for the phenol–formaldehyde reaction belongs to a wider class of kinetic networks made up of irreversible nonchain reactions. In this section, a general form of the mathematical model for this class of reactive systems is presented; moreover, it is shown that the temperature attainable in the reactor is bounded and the lower and upper bounds are computed.

To this goal, let us consider a cooled batch reactor in which the following network of irreversible reactions takes place:

$$
\begin{array}{llll}
\mathrm{A}_1 \longrightarrow \upsilon_{1,2}\mathrm{A}_2 & & & \\
\mathrm{A}_1 \longrightarrow \upsilon_{1,3}\mathrm{A}_3 & \mathrm{A}_2 \longrightarrow \upsilon_{2,3}\mathrm{A}_3 & & \\
\vdots & \vdots & & \\
\mathrm{A}_1 \longrightarrow \upsilon_{1,N_\mathrm{C}+1}\mathrm{A}_{N_\mathrm{C}+1} & \mathrm{A}_2 \longrightarrow \upsilon_{2,N_\mathrm{C}+1}\mathrm{A}_{N_\mathrm{C}+1} & \ldots & \mathrm{A}_{N_\mathrm{C}} \longrightarrow \upsilon_{N_\mathrm{C},N_\mathrm{C}+1}\,\mathrm{A}_{N_\mathrm{C}+1}
\end{array}
$$

where A_i denotes the ith component, $\upsilon_{i,j} \geq 0$ is the stoichiometric coefficient of A_j in the reaction $\mathrm{A}_i \rightarrow \mathrm{A}_j$, and $\mathrm{A}_{N_\mathrm{C}+1}$ is the final product. The above mechanism represents a general scheme of irreversible nonchain reactions involving N_C reactants and can be reduced to a simpler series and/or parallel reaction scheme by assuming $\upsilon_{i,j} = 0$ for the reactions to be eliminated.

Table 2.5 Condensation reactions producing the dimers DPh_2

No.	Reaction	k_0 [$m^3\,mol^{-1}\,s^{-1}$]
33	Ph + TMPh → 2,4-M-1,6-MDPh	$7.38 \cdot 10^3$
34	Ph + TMPh → 2,4-M-1,8-MDPh	$6.10 \cdot 10^3$
35	Ph + TMPh → 7,9-M-1,8-MDPh	$8.57 \cdot 10^3$
36	Ph + TMPh → 2,4-M-3,8-MDPh	$7.08 \cdot 10^3$
37	1-MPh + 1,5-MPh → 2,7-M-1,6-MDPh	$4.32 \cdot 10^3$
38	1-MPh + 1,5-MPh → 7,9-M-1,8-MDPh	2.39
39	1-MPh + 1,5-MPh → 2,7-M-1,8-MDPh	$6.92 \cdot 10^4$
40	1-MPh + 1,3-MPh → 2,4-M-1,6-MDPh	$7.86 \cdot 10^3$
41	1-MPh + 1,3-MPh → 2,9-M-1,6-MDPh	$2.50 \cdot 10^2$
42	1-MPh + 1,3-MPh → 4,7-M-1,8-MDPh	$4.00 \cdot 10^3$
43	1-MPh + 1,3-MPh → 2,7-M-1,8-MDPh	$3.19 \cdot 10^2$
44	1-MPh + 1,3-MPh → 2,7-M-3,8-MDPh	$5.12 \cdot 10^3$
45	3-MPh + 1,5-MPh → 2,4-M-3,8-MDPh	1.52
46	3-MPh + 1,5-MPh → 2,9-M-1,6-MDPh	$9.29 \cdot 10^4$
47	3-MPh + 1,3-MPh → 4,9-M-1,6-MDPh	$5.37 \cdot 10^3$
48	3-MPh + 1,3-MPh → 2,4-M-1,8-MDPh	$4.98 \cdot 10^3$
49	3-MPh + 1,3-MPh → 4,7-M-1,8-MDPh	$6.87 \cdot 10^3$
50	1-MPh + TMPh → 2,4-M-1,6-MDPh + F	$2.93 \cdot 10^3$
51	1-MPh + TMPh → 7,9-M-1,8-MDPh + F	$3.40 \cdot 10^3$
52	3-MPh + TMPh → 2,4-M-1,8-MDPh + F	$1.86 \cdot 10^3$
53	3-MPh + TMPh → 2,4-M-3,8-MDPh + F	$2.15 \cdot 10^3$
54	1,5-MPh + 1,5-MPh → 2,7-M-1,6-MDPh + F	$8.26 \cdot 10^4$
55	1,3-MPh + 1,5-MPh → 2,9-M-1,6-MDPh + F	$4.78 \cdot 10^3$
56	1,3-MPh + 1,5-MPh → 2,7-M-1,8-MDPh + F	$6.10 \cdot 10^3$
57	1,3-MPh + 1,3-MPh → 4,9-M-1,6-MDPh + F	$2.76 \cdot 10^2$
58	1,3-MPh + 1,3-MPh → 4,7-M-1,8-MDPh + F	$7.06 \cdot 10^2$
59	1,3-MPh + 1,3-MPh → 2,7-M-3,8-MDPh + F	$4.51 \cdot 10^2$

Assuming first-order kinetics and perfect mixing of the reactor contents, the mass balances are

$$\begin{aligned}
\dot{C}_1 &= -k_{c1}(T_r)C_1,\\
\dot{C}_2 &= \upsilon_{1,2}k_{c1,2}(T_r)C_1 - k_{c2}(T_r)C_2,\\
\dot{C}_3 &= \upsilon_{1,3}k_{c1,3}(T_r)C_1 + \upsilon_{2,3}k_{c2,3}(T_r)C_2 - k_{c3}(T)C_3,\\
&\vdots\\
\dot{C}_{N_C} &= \upsilon_{1,N_C}k_{c1,N_C}(T_r)C_1 + \cdots\\
&\quad + \upsilon_{N_C-1,N_C}k_{cN_C-1,N_C}(T_r)C_{N_C-1} - k_{cN_C}(T_r)C_{N_C},
\end{aligned} \tag{2.27}$$

Table 2.6 Condensation reactions producing the dimers DPh_3

No.	Reaction	k_0 [$m^3\ mol^{-1}\ s^{-1}$]
60	1-MPh + TMPh → 2,4,7-M-1,6-MDPh	$1.16 \cdot 10^3$
61	1-MPh + TMPh → 2,4,7-M-1,8-MDPh	$1.85 \cdot 10^4$
62	1-MPh + TMPh → 2,7,9-M-1,8-MDPh	$1.34 \cdot 10^3$
63	1-MPh + TMPh → 2,4,7-M-3,8-MDPh	$2.15 \cdot 10^4$
64	3-MPh + TMPh → 2,4,9-M-1,6-MDPh + F	$2.49 \cdot 10^3$
65	3-MPh + TMPh → 4,7,9-M-1,8-MDPh + F	$2.89 \cdot 10^3$
66	1,5-MPh + 1,5-MPh → 2,7,9-M-1,8-MDPh	$3.61 \cdot 10$
67	1,5-MPh + 1,3-MPh → 2,4,7-M-1,6-MDPh	$5.93 \cdot 10^4$
68	1,5-MPh + 1,3-MPh → 4,7,9-M-1,8-MDPh	1.05
69	1,5-MPh + 1,3-MPh → 2,4,7-M-3,8-MDPh	1.34
70	1,3-MPh + 1,3-MPh → 2,4,9-M-1,6-MDPh	$6.87 \cdot 10^3$
71	1,3-MPh + 1,3-MPh → 2,4,7-M-1,8-MDPh	$8.78 \cdot 10^3$
72	1,5-MPh + TMPh → 2,4,7-M-1,6-MDPh + F	$2.21 \cdot 10^4$
73	1,5-MPh + TMPh → 2,7,9-M-1,8-MDPh + F	$2.68 \cdot 10^3$
74	1,3-MPh + TMPh → 2,4,9-M-1,6-MDPh + F	$1.28 \cdot 10^3$
75	1,3-MPh + TMPh → 2,4,7-M-1,8-MDPh + F	$1.64 \cdot 10^3$
76	1,3-MPh + TMPh → 4,7,9-M-1,8-MDPh + F	$1.49 \cdot 10^3$
77	1,3-MPh + TMPh → 2,4,7-M-3,8-MDPh + F	$1.90 \cdot 10^3$

Table 2.7 Condensation reactions producing the dimers DPh_4

No.	Reaction	k_0 [$m^3\ mol^{-1}\ s^{-1}$]
78	1,5-MPh + TMPh → 2,4,7,9-M-1,8-MDPh	4.48
79	1,5-MPh + TMPh → 2,4,7,9-M-3,8-MDPh	5.62
80	1,3-MPh + TMPh → 2,4,7,9-M-1,6-MDPh	$1.59 \cdot 10^4$
81	1,3-MPh + TMPh → 2,4,7,9-M-1,8-MDPh	$1.85 \cdot 10^4$
82	TMPh + TMPh → 2,4,7,9-M-1,6-MDPh + F	$5.93 \cdot 10^3$
83	TMPh + TMPh → 2,4,7,9-M-1,8-MDPh + F	$1.38 \cdot 10^4$
84	TMPh + TMPh → 2,4,7,9-M-3,8-MDPh + F	$7.98 \cdot 10^3$

where C_i $(i = 1, \ldots, N_C)$ is the concentration of the chemical species A_i, T_r is the reactor temperature, $k_{ci,j}$ $(j = 2, \ldots, N_C)$ is the rate constant of the reaction $A_i \rightarrow A_j$, following the Arrhenius law

$$k_{ci,j}(T_r) = k_{0i,j} \exp\left(-\frac{E_{ai,j}}{\mathcal{R}T_r}\right), \tag{2.28}$$

$E_{ai,j}$ is the activation energy of each reaction, and $k_{0i,j}$ is the corresponding preexponential factor. Moreover, the lumped rate constant k_{ci} of the reactions of disap-

Table 2.8 Addition reactions of formaldehyde to a dimer

No.	Reaction	k_0 [m^3 mol^{-1} s^{-1}]
85	$DPh_0 + F \rightarrow DPh_1$	$1.40 \cdot 10^5$
86	$DPh_1 + F \rightarrow DPh_2$	$2.41 \cdot 10^5$
87	$DPh_2 + F \rightarrow DPh_3$	$2.20 \cdot 10^5$
88	$DPh_3 + F \rightarrow DPh_4$	$2.52 \cdot 10^5$

pearance of species i is defined as

$$k_{ci}(T_r) = \sum_{j=i+1}^{N_C+1} k_{ci,j}(T_r). \tag{2.29}$$

In order to write the heat balance, it is assumed that all reactions are exothermic, that the temperature control is achieved by means of a heat exchange jacket surrounding the reactor, and that heat losses to the environment can be neglected. Energy balances can be written both for the fluid in the reactor and for the fluid in the jacket. In the first case, by including in (2.25) the proper expression for the total heat of reaction, this equation reads

$$\dot{T}_r = \frac{\sum_{i=1}^{N_C} \sum_{j=i+1}^{N_C+1} (-\Delta H_{Ri,j}) k_{ci,j}(T_r) C_i}{\rho_r c_r} - \frac{U S (T_r - T_j)}{\rho_r c_r V_r}, \tag{2.30}$$

where $\Delta H_{Ri,j}$ denotes molar enthalpy change of each reaction.

In the second case, for the sake of simplicity, the jacket is modeled as a continuous well-mixed vessel, so that the general framework of the mass balance for a CSTR (2.23) can be adequately rearranged to give

$$\dot{T}_j = \frac{F_V (T_{in} - T_j)}{V_j} + \frac{U S (T_r - T_j)}{\rho_j c_j V_j}, \tag{2.31}$$

where the subscript j denotes variables referred to the jacket, F_V and T_{in} are the volume flow rate and the temperature of the fluid entering the jacket, respectively.

All the stages of the reaction cycle (i.e., initial reactor heating, reaction development, and final quenching) can be described by (2.30) and (2.31). Indeed, the second term on the right-hand side of (2.30) usually turns out to be negative during the heating phase (when $T_{in} > T_j > T_r$) and positive during temperature control and final cooling ($T_{in} < T_j < T_r$).

It can be easily recognized that the rate constants are nonnegative and strictly increasing functions of the reactor temperature T_r. Since the reaction is assumed to be exothermic and T_{in} is bounded, i.e., $T_{in,min} \leq T_{in} \leq T_{in,max}$, the temperature in the reactor is lower bounded by the value

$$T_{r,min} = \min\{T_{r,0}, T_{j,min}\},$$

where $T_{r,0}$ is the initial reactor temperature, and $T_{j,min}$ is the minimum attainable jacket temperature, which coincides with the minimum attainable value, $T_{in,min}$, of T_{in}. Moreover, extending the concept of adiabatic reaction temperature introduced in Sect. 2.3.2, an upper bound for T_r can be computed by considering the ideal heating/reaction scheme composed by the following two steps:

- the reacting mixture is first heated up to the maximum temperature value, $T_{in,max}$, of the fluid entering the jacket; and
- then the complete reactants conversion takes place adiabatically.

The numerical value of the upper bound is given by

$$T_{r,max} = T_{in,max} + C_{10} \frac{(-\Delta H_{R1,N_C+1})}{\rho_r c_{pr}},$$

where C_{10} is the initial concentration of A_1. As a consequence, the rate constants are also bounded as follows:

$$0 < \underline{k}_{ci,j} \leq k_{ci,j}(T_r) \leq \overline{k}_{ci,j} \quad \forall\, T_r,\ i = 1, \ldots, N_C,\ j = i+1, \ldots, N_C+1, \tag{2.32}$$

where $\underline{k}_{ci,j} = k_{ci,j}(T_{r,min})$ and $\overline{k}_{ci,j} = k_{ci,j}(T_{r,max})$.

In view of inequalities (2.32), also the lumped rate constants k_{ci} can be bounded as follows:

$$0 < \underline{k}_{ci} \leq k_{ci}(T_r) \leq \overline{k}_{ci} \quad \forall T_r,\ i = 1, \ldots, N_C, \tag{2.33}$$

where $\underline{k}_{ci} = \sum_{j=i+1}^{N_C+1} \underline{k}_{ci,j}$ and $\overline{k}_{ci} = \sum_{j=i+1}^{N_C+1} \overline{k}_{ci,j}$.

These results will be used in Chap. 5 when dealing with model-based control of nonchain reactions in a cooled batch reactor.

2.6 Measuring the Reactor Status

The modeling approach to the batch reactor presented in the previous sections of this chapter must be strengthened and extended by considering the relationship between the user and the reactor. This relationship may be divided into two different parts, namely the methods for measuring the reactor status and the actions to be taken in order to change it.

Measuring the variables which define the reactor status is important both in the laboratory and in the industrial practice. In the first case, measuring gives the experimental information necessary to tune the mathematical models, i.e., to determine the values of the adjustable parameters, a task to whom the entire Chap. 3 is devoted. In industry, measuring and regulating the operative conditions is very important in order to ensure an adequate quality of the final product and safe operation of the batch cycle. These two ways of using measurements pose different problems to the user, because they require different properties of the measurement device. Thus, before considering in some detail the main measurable variables, a short review of the measuring qualities is deemed to be useful.

2.6.1 Measurements Quality

In a few simpler cases, the use of very basic measuring instruments involves the direct comparison of the physical quantity to be measured with predisposed samples and scales, as happens, for example, when measuring a length with a ruler. On the contrary, almost all the measurements of industrial interest are obtained by means of a more complex measuring instrument, which is a device that translates some physical effect depending on the measurable quantity in a signal usable at the user interface.

In general, the relationship between input and output of a measuring instrument is a complex function that must be determined by calibration, i.e., by recording the output corresponding to different known values of the input, so that a *calibration curve* can be obtained. In most cases, the functionality represented by the calibration curve is a mere interpolation of experimental points rather than a predetermined theoretical law. The slope of the calibration curve defines the *sensitivity* of the measuring instrument; in general, the higher the sensitivity, the more accurate is the measurement.

The quality of measurements is determined by a compromise between costs and process reliability and can be described in terms of accuracy, precision or repeatability, resolution, response time, and stability. The first two properties are strictly related to the concept of measurement error, which can never be completely eliminated. The *accuracy* of a measuring instrument is the ability to provide outputs which are, on average, close to the true value of the underlying variable. The *precision* (or repeatability) of a measuring instrument is the ability to replicate the measured values under the same conditions and corresponds to the standard deviation of the errors. The *resolution* is the ability of a measuring system to detect small changes in the measured variable; the smaller the changes detected by the instrument, the higher its resolution. The *response time* of an instrument can be defined as the time needed to let the instrument output settle around the measured value for an input step change. Finally, *stability* (or ruggedness) is the ability of a sensor to maintain its performance under the expected operative conditions.

2.6.2 Online Measurements

In order to ensure an adequate quality of products and a safe operation, the monitoring of a batch reactor should include, at least, online measurements of temperature, pressure, and of some composition-related variables. In this context, online measurements may be defined as measurements obtained via instruments strictly connected to the reactor and characterize by response times markedly smaller than the characteristic times of the chemical reaction. In general, this is the case of temperature and pressure, which can be easily measured online by means of reliable, relatively cheap, and poorly intrusive sensors. This allows the introduction of sensor redundancy, a common practice to increase reliability. On the other hand, online

Table 2.9 Comparison of RTD and thermocouple characteristics

	RTD	Thermocouple
Temperature Range [°C]	−200 to 850	−200 to 1800
Accuracy [°C]	10^{-4}–10^{-2}	0.1–2
Response Time [s]	0.5–5	0.01–1
Stability	High	Moderate
Sensitivity	High	Low
Cost	Moderate	Low

measurements of chemical composition is a more challenging task, especially in liquid systems, so that indirect measurements through composition related overall properties (e.g., pH) often represent the only viable alternative.

Temperature is by far the more frequently measured state variable and is considered in some detail hereafter. Basic temperature measurement in a batch reactor must regard, at least, the reacting mixture and the heat exchange fluid. To this goal, the devices most widely used are thermocouples and resistance temperature detectors (RTD).

Thermocouples are based on the thermoelectric Seebeck effect, which generates a voltage at the junction between two metallic conductors, which depends on temperature [13]. Thus, in the measuring circuit, two junctions are created, namely, a sensitive (or hot) junction at the point where temperature has to be measured and a nonsensitive (cold) junction, kept at a constant known temperature, where the voltage established between the conductors can be easily measured [19]. Different typologies of thermocouples exist for application in a wide range of conditions; they essentially differ by the materials, the most common being J (iron/constantan), K (chromel/alumel), T (copper/constantan), and E (chromel/constantan).

RTD sensors consist of a platinum (with copper and nickel being cheaper alternatives) wire wrapped in a coil and traversed by a constant current, typically in the range 0.8–1.0 mA. Since the electric resistance of these materials changes almost linearly with temperature at a rate of about $0.3\%\,°C^{-1}$, the voltage drop across the sensor is easily converted into a temperature value. Accuracy of RTDs is on average higher than that of thermocouples, and platinum-based resistive detectors can be as accurate as 10^{-4}°C [19]. On the other hand, their response time is somewhat larger, because of the time needed by the measuring coil to reach thermal equilibrium with the surroundings. A good alternative to RTDs are thermistors, based on the resistance sensitivity of semiconductors with respect to temperature.

Comparison of RTD and thermocouple average performance is reported in Table 2.9. Here, the response time is defined as the time needed by the device to reach the final temperature within 0.5% of its value for a temperature step change.

Besides the electrical devices described above, mechanical systems for temperature measurement are not uncommon in chemical reactors. As an example, systems consisting in a bulb connected to a temperature-sensitive volume or pressure ele-

ment can occasionally offer some interesting advantages, e.g., independence from external electrical power and simpler maintenance [2].

The optimal location of temperature sensors is not a trivial task, because, in industrial scale chemical reactors, temperature gradients can be generated by nonperfect mixing and by the heat exchange device. In systems that are very sensitive to temperature (as in the case of the phenol–formaldehyde reaction introduced in Sect. 2.4), the temperature should be measured in the hottest point (*hot spot*), a strategy which proves to be too conservative when safety is not an issue, since the reaction rate in the remaining parts of the reactor could prove to be rather slow. Moreover, it should be considered that the hot spots may move within the reactor according to the different stages of operation.

A similar problem affects the heat exchange jacket and may be reduced by using a coil, in which a plug flow can be assumed for the heat exchange fluid. When the reaction temperature is controlled by an external heat exchanger or condenser [17], the recirculation of the fluids introduces a transport delay that may strongly affect the control action.

It is also interesting to briefly consider online measurements of variables different from temperature [5]. Since pressure is defined as the normal force per unit area exerted by a fluid on a surface, the relevant measurements are usually based on the effects deriving from deformation of a proper device. The most common pressure sensors are piezoresistive sensors or strain gages, which exploit the change in electric resistance of a stressed material, and the capacitive sensors, which exploit the deformation of an element of a capacitor. Both these sensors can guarantee an accuracy better than 0.1 percent of the full scale, even if strain gages are temperature sensitive.

Pressure is more directly connected to the concept of explosion; nevertheless, it is less directly connected to the reactor status, since, for liquid-phase reactors, pressure nonlinearly depends on temperature (trough the vapor pressure relationship) and concentration (through the activity coefficients in liquid phase). Moreover, since pressure measurements are usually less accurate than temperature measurements, they are to be considered in particular for gassy reactions, i.e., when the runaway produces small temperature effects but large amounts of incondensable products in gaseous phase.

Online measurements of composition would be very appreciated, because composition is the most important variable. Unfortunately, direct measurements of the amount of a single component can be obtained only in a few cases, and typically for gaseous system, an example being the measurement of oxygen based on its paramagnetism. In fact, liquid phase systems are usually made out of components of similar chemical structure, and these must be separated before measuring their quantity.

Thus, online measurements of composition are usually limited to some overall property. A typical example is pH, defined as the absolute value of the logarithm of the molar concentration (or, more exactly, activity) of hydrogen ion; pH can be measured by exploiting the electric potential established between two proper electrodes immersed in the sample fluid, usually a glass membrane electrode and a reference electrode [15]. Notwithstanding the temperature dependence and the alkaline error (at high pH, a marked sensitivity to the effect of Na^+ and of other monovalent

cations), accuracies of 0.01–0.1 pH units can be achieved. Alternatively, electric conductivity and optical density may give some online information about composition [1].

Finally, one can easily obtain the properties of the stirring system (rotational speed and torque) and compute the stirring power from their product, but these variables are only indirectly linked to the reactor status through the system density.

2.6.3 Offline Measurements

An offline measurement apparatus is usually not directly mounted on the reactor, but is fed with samples withdrawn from it manually or automatically. This is the typical case of chromatography, a widely used measurement device for gas and liquid composition. Both gas and liquid chromatographies are based on the separation of the sample by means of selective adsorption on a solid substrate posed in a fixed bed column, and on the detection of the change of a suitable property of the (gas or liquid) carrier, usually thermal conductivity.

It appears that each component is characterized by a retention time (which also depends on the substrate and on the column length and temperature) and by a relationship between its amount and the thermal conductivity of the modified carrier. Therefore, not only a calibration curve is required for any component, but also the operating conditions must be optimized in order to obtain a sharp separation among the different components.

In conclusion, a complete analysis of a complex mixture can require very long times (from a few minutes up to many hours); thus, such a measuring apparatus is not suited for online measurements to be used in reactor control. On the contrary, in the laboratory, chromatography is very often the preferred method of analysis of complex mixtures, since these more accurate data can be used to identify the reaction mechanism and the relevant kinetic parameters.

This brief overview of offline measurements can be concluded by considering the measurements of the heat released by chemical reactions, which can be obtained via calorimetric measurements [7, 18]. The most diffused industrial calorimeters are the so-called reaction calorimeters, basically consisting in jacketed vessels in which the reaction takes place and the heat released is measured by monitoring the temperature of the fluid in the jacket. A class of alternative instruments are the scanning calorimeters (differential or adiabatic), in which the analysis is performed by linearly increasing the sample temperature with respect to time, in order to test the reactivity of potentially unstable chemical systems in a proper temperature range by measuring the released heat.

2.7 Manipulating the Reactor Status

Chemical reactions proceed at very different reaction rates, so that typical values of characteristic reaction time in industrial batch reactors range from few hours to

several days. The largest values are encountered in chemical systems like polymerization reactions, the smallest in some biological reactions such as fermentation of sugars to alcohols. Thus, a challenging problem of automatic control is met in the first case, whereas, in the second case, the reaction is often controlled manually, and the problem is restricted to selecting the best action to be executed in a given state of the process.

In both cases, it is of interest to single out the variables that can be manipulated; it is possible to distinguish the actions scheduled in the design of the process, the actions aimed at controlling the reactor in the presence of failures, and the emergency actions to be operated in the case of runaway.

In general, it does not make much sense to modify the speed of the mechanical stirrer, since its design value is fixed to optimize the mixing of the reactor contents and the value of the heat transfer coefficient. On the contrary, it is possible to modify the reaction rate and consequently the temperature by adding to the reacting mixture a proper amount of fresh solvent, and/or of a reactant, a catalyst, or a reaction inhibitor.

In many cases, these operations are scheduled as standard operating procedures; nevertheless, the addition of fresh solvent and/or of a reaction inhibitor can be also used as an emergency protection measure against explosions. This suppression system should be preferred to the alternative method consisting in a bursting disc, which must be provided with a discharge line to an emergency tank, since the discharge into the environment of the reactor contents must be avoided. In fact, the design of the discharge line in the presence of unsteady two-phase flashing flow is not straightforward, whereas the only drawback of a suppressing system is the need for allowing a larger gaseous head in the reactor.

In this book, automatic control of reactor temperature is the most interesting target; to this purpose, the manipulated variable is usually one (or a combination of) the following [3]:

- the flow rate of the heat exchange fluid
- the inlet temperature of the heat exchange fluid; and
- the heat exchange surface.

The first strategy appears to be very effective; in fact, as shown by (2.30) and (2.31), the direct (linear) effect of increasing the flow rate is augmented by the increase of the jacket-side heat exchange coefficient. This control action can be realized without a noticeable time delay by a simple control valve, the only drawback for its quantitative assessment being the nonlinear relationship between the overall heat exchange coefficient and the flow rate of the heat exchange fluid.

The inlet temperature of the heat exchange fluid has a more easily predictable effect on the system dynamics (in fact, the small change of the heat transfer coefficient with temperature is usually negligible) and is therefore preferred in model-based control approaches. The implementation of this strategy requires the availability of two compatible heat exchange fluids (usually water for cooling and steam for heating) and of a mixing device for conditioning the heat exchange fluid at the required flow rate and temperature, which introduces a time delay in the system.

Finally, the choice of the heat exchange surface area as adjustable parameter is a recent concept developed after the diffusion of cooling systems partitioned into separated compartments. By controlling the corresponding opening/closing valves, heat exchange compartments can be excluded or joined, whereas inlet temperature and flow rates are kept constant. In this way, the exchange surface can be adjusted according to the degree of filling of the reactor and to the heat exchange flux required for temperature control. Other advantages are the fast response of the cooling system to the control action and the absence of a pronounced cold/hot region at the reactor wall since the coolant inlets are manifold. Drawbacks of this configuration are the higher pressure drops and the more complex flow patterns of the heat exchange fluid, which affect the modeling approach.

2.8 Conclusions

The modeling of chemical batch reactors has been chosen as the starting point for the roadmap developed in this book. The simplified mathematical models presented in the first sections of the chapter allow us to focus the attention on different aspects of chemical kinetics, whereas the causes of nonideal behavior of chemical batch reactors are faced in the last chapter.

The rather complex issue of chemical kinetics has been discussed in a quantitative way, in order to stress out two main ideas, namely, the necessity of resorting to simplified kinetic models and the need of adequate methods of data analysis to estimate the kinetic parameters. These results introduce Chap. 3, in which basic concepts and up-to-date methods of identification of kinetic parameters are presented.

To this purpose, a brief overview of the measurable variables in a batch reactor has been included; the difference between online measurements, suitable for control purposes, and offline measurements, which can be exploited to obtain experimental data to be used for the identification, has been stressed.

In the second part of the chapter, the mathematical model of the BR has been augmented by considering its behavior in the presence of significant thermal effects and of a proper heat exchange apparatus. In particular, modeling these aspects brings the reader to understand the need for considering the thermal stability of batch reactors (Chap. 4) and the need for adequate systems of automatic temperature control (Chap. 5).

References

1. J.H. Altman. Densitometry measurements. In J.C. Webster, editor, *Measurement, Instrumentation, and Sensors Handbook*, *2nd Edition*, Chap. 57. CRC Press, Boca Raton, 1999.
2. N.A. Anderson. *Instrumentation for Process Measurement and Control*. CRC Press, Boca Raton, 1998.
3. D. Bonvin. Optimal operation of batch reactors—a personal view. *Journal of Process Control*, 8(5/6):355–368, 1998.

4. M. Buback and A.M. van Herk. *Radical Polymerization: Kinetics and Mechanism*. Wiley-VCH, Weinheim, 2007.
5. K.H.L. Chau, R. Goehner, E. Drubetsky, H.M. Brady, W.H. Bayles, Jr., and P.C. Pedersen. Pressure and sound measurement. In J.C. Webster, editor, *Measurement, Instrumentation, and Sensors Handbook*, *2nd Edition*, Chap. 26. CRC Press, Boca Raton, 1999.
6. I. Chorkendorff and J.W. Niemantsverdriet. *Concept of Modern Catalysis and Kinetics*. Wiley-VCH, Weinheim, 2003.
7. J.A. Dean. *The Analytical Chemistry Handbook*. McGraw Hill, New York, 1995.
8. K.C. Eapen and L.M. Yeddenapalli. Kinetics and mechanism of the alkali-catalyzed addition of formaldehyde to phenol and substituted phenols. *Die Makromolekulare Chemie*, 119(2766):4–16, 1968.
9. W. Hesse. Phenolic resins. In *Ullmann's Encyclopedia of Industrial Chemistry*, *6th Edition*. Wiley, New York, 2001.
10. O. Levenspiel. *Chemical Reaction Engineering*, *3rd Edition*. Wiley, New York, 1999.
11. L.B. Manfredi, C.C. Riccardi, O. de la Osa, and A. Vazquez. Modelling of resol resin polymerization with various formaldehyde/phenol molar ratios. *Polymer International*, 50:796–802, 2001.
12. J. Nielsen, J. Villadsen, and G. Lidén. *Bioreaction Engineering Principles*, *2nd Edition*. Kluwer Academic, New York, 2003.
13. R.P. Reed. Thermal effects in industrial electronics circuits. In J.D. Irwin, editor, *Industrial Electronics Handbook*. CRC Press, Boca Raton, 1996.
14. C.C. Riccardi, G. Astarloa Aierbe, J.M. Echeverria, and I. Mondragon. Modelling of phenolic resin polymerisation. *Polymer*, 43:1631–1639, 2002.
15. N.F. Sheppard, Jr. and A. Giuseppi-Elie. PH measurements. In J.C. Webster, editor, *Measurement, Instrumentation, and Sensors Handbook*, *2nd Edition*. Chap. 71. CRC Press, Boca Raton, 1999.
16. G.P. Smith, D.M. Golden, M. Frenklach, N.W. Moriarty, B. Eiteneer, M. Goldenberg, C.T. Bowman, R.K. Hanson, S. Song, W.C. Gardiner Jr., V.V. Lissianski, and Z. Qin. GRI-Mech 3.0. A kinetic mechanism to model natural gas combustion. www.me.berkley.edu/grimech/.
17. P. Trambouze and J.-P. Euzen. *Chemical Reactors: From Design to Operation*. Editions Technip, Paris, 2004.
18. S. van Herwaarden. Calorimetry measurement. In J.C. Webster, editor, *Measurement, Instrumentation, and Sensors Handbook*, *2nd Edition*, Chap. 36. CRC Press, Boca Raton, 1999.
19. J.G. Webster, editor. *Measurement, Instrumentation, and Sensors Handbook*. CRC Press, Boca Raton, 1999.

http://www.springer.com/978-0-85729-194-3

Control and Monitoring of Chemical Batch Reactors

Caccavale, F.; Iamarino, M.; Pierri, F.; Tufano, V.

2011, XVII, 186 p., Hardcover
ISBN: 978-0-85729-194-3